Catal Lett (2009) 129:486–492
DOI 10.1007/s10562-008-9827-4

Study on Methanethiol Synthesis from H_2S-Rich Syngas Over K_2MoO_4 Catalyst Supported on Electrolessly Ni-Plated SiO_2

Yingjuan Hao · Yuanhua Zhang · Aiping Chen ·
Weiping Fang · Yiquan Yang

Received: 13 November 2008 / Accepted: 13 December 2008 / Published online: 21 January 2009
© Springer Science+Business Media, LLC 2009

Abstract Small amount of Nickel deposited on SiO_2 support by electroless plating was verified to have a significant promoting effect on the catalytic performance of the K_2MoO_4/SiO_2 catalyst for methanethiol synthesis from H_2S-rich synthesis gas. The addition of Nickel was found to be in favor of the suppression of the CO_2 formation. The results of BET, TPR and Raman characterizations for the Ni-modified SiO_2 and the catalyst K_2MoO_4/Ni-SiO_2 showed that the surface properties of Ni-modified SiO_2 were similar to those of unmodified SiO_2 and that no Raman characteristic band specific to NiO from the catalyst K_2MoO_4/Ni-SiO_2 was detected. For oxidic K_2MoO_4/Ni-SiO_2 catalyst lower reduction temperature was measured. For sulfided catalysts, reduced molybdenum oxides and oxysulfides were detected, which was inferred to be closely related to high catalytic activity of the catalyst.

Keywords Methanethoil · K_2MoO_4 · Electroless plating nickel · TPR · LRS

1 Introduction

Methanethoil is an important chemical intermediate widely used to produce a variety of agricultural chemicals, in particular, methionine, a widely used feed supplement for poultry [1, 2]. The synthesis of methanethoil from carbon oxides (CO or CO_2), hydrogen and hydrogen sulfide over supported catalysts has been widely investigated since 1980s [1–9]. The catalyst system used in the literature was composed of an active component molybdenum or tungsten with an alkali metal as a promoter and an oxide support. Some transition metals and rare earth metals such as iron, cobalt, nickel, zinc, manganese and cerium are often chosen to be active additives [2]. It is known that the activity of the catalyst depends not only on the extent of the dispersed molybdate oxide and promoter (nickel or cobalt) oxide but also on the nature of the support and the preparation method used [10].

Recently, electroless plating technique has been widely applied to the catalysis fields. Tsai et al. [11] have investigated the catalytic effects of the Ni–P alloy on Si wafer for the growth of carbon nanofibers and also studied the effects of nickel on the initial growth behavior of electroless Ni–Co–P alloy on silicon substrate [12]. Dai et al. have investigated high-performance of cobalt–tungsten–boron catalyst supported on Ni foam for hydrogen generation from alkaline sodium borohydride solution [13].

In this paper a small amount of Ni promoter was deposited onto SiO_2 by electroless plating to obtain Ni-SiO_2 support, on which the active component K_2MoO_4 was then impregnated to prepare the catalyst K_2MoO_4/Ni-SiO_2 for methanethiol synthesis from H_2S-rich synthesis gas. The promoting effect of Nickel thus deposited onto SiO_2 on the catalytic performance of the catalyst for the reaction and the active species of the catalyst K_2MoO_4/Ni-SiO_2 were investigated.

2 Experimental

2.1 Catalyst Preparation

Ni-modified SiO_2 support was prepared by electroless plating method [12]. Desired amount of commercial SiO_2

Y. Hao · Y. Zhang · A. Chen · W. Fang · Y. Yang (✉)
Department of Chemistry, College of Chemistry and Chemical Engineering, Xiamen University, 361005 Xiamen, People's Republic of China
e-mail: yyiquan@xmu.edu.cn

was washed with distilled water, and then dried, followed by immersing the washed SiO_2 in a mixing solution of H_2SO_4 (4.5 mol/L) plus H_2O_2 (0.88 mol/L) (1:1 by volume) for 5 min under agitating. The cleaned SiO_2 obtained was then immersed in a $PdCl_2/HCl$ (0.1 g/L) solution for 10 min for activation, followed by washing with distilled water again. Finally, the activated SiO_2 was put into a plating solution to be electrolessly plated. The composition of the plating solution is listed in Table 1. After 30 min plating, the Ni-modified support obtained was dried at 383 K for 10 h and denoted as Ni-SiO_2. The nickel contents of Ni-SiO_2 were also showed in Table 1.

The catalysts K_2MoO_4/SiO_2 and K_2MoO_4/Ni-SiO_2 were prepared by means of incipient wetness impregnation [14]. Suitable amount of SiO_2 or Ni-SiO_2 prepared by electroless plating was soaked in an aqueous solution of K_2MoO_4 with $NH_3 \cdot H_2O$ adjusting the pH of the solution at 9, after an overnight impregnating, the wet catalyst was dried at 383 K for 10 h to generate a catalyst denoted as K_2MoO_4/SiO_2 or K_2MoO_4/Ni-SiO_2. The fractions of K_2MoO_4 and Ni were, respectively, determined by comparing the amounts of K_2MoO_4 (expressed by the amount of MoO_3) and Ni with that of SiO_2 which was set to be 100.

2.2 Activity Testing

The catalyst performance was evaluated in a stainless steel tubular reactor filled with 5 mL of the catalyst per pass. The evaluation experiments were performed under the reaction conditions of 0.2 MPa, 573 K, feed gas mixture $CO:H_2:H_2S = 1:1:2$ (by volume) and GHSV = 2,000 h^{-1}. Hydrocarbon, sulfur-containing products and CO or CO_2 were analyzed by on-line GC equipped with flame ionization detector (GDX-103 column, 1.5 m × ϕ8 mm), flame photometric detector (HP-Plot/Q capillary column, 30 m × 0.54 mm × 40 μm) and thermal conductivity detector (carbon molecular sieves column, 1.5 m × ϕ8 mm), respectively, [14].

Table 1 chemical composition of the plating solution and Ni content in Ni-SiO_2 support obtained

Chemical composition	Concentration (g/L)					
	1#	2#	3#	4#	5#	6#
Chemical composition of the plating solution						
$NiSO_4 \cdot 6H_2O$	1.3	2.5	5.0	7.5	10.0	12.5
$Na_3C_3H_6O_7$	1.3	2.5	5.0	7.5	10.0	12.5
$NaH_2PO_2 \cdot H_2O$	2.0	3.8	7.5	10.0	12.5	15.0
$(NH_4)_2 \cdot SO_4$	2.0	3.8	7.5	10.0	12.5	15.0
Ni content of Ni-SiO_2 support obtained						
Ni-SiO_2 (wt%)	0.10	0.21	0.49	0.71	0.91	1.17

2.3 Catalyst Characterization

BET surface area, pore size and pore volume of both the catalysts and the supports were measured by using an adsorption equipment Nova4000e.

TPR experiments of both the catalysts and the supports were carried out in a quartz tube filled with 60 mg of sample per run. The heating rate of 10 K/min in a temperature range from 323 to 1,073 K was adopted under a gas mixture of 5% H_2 in argon at a flow of 20 mL/min. H_2 consumption during TPR experiments was monitored with a thermal conductivity detector (TCD).

Raman spectra were recorded on a computer-controlled Renishaw Invia Spectrometer system, using 532 nm argon-ion laser as an exciting source. The spectra resolution was 2 cm^{-1} and laser power was 20 mW. All the Raman spectra were recorded under ambient conditions.

3 Results and Discussion

3.1 Catalytic Performance Study

The catalytic performances of the K_2MoO_4/Ni-SiO_2 catalysts with different Ni loadings for methanethiol synthesis from H_2S-rich synthesis gas are shown in Table 2. Table 2 shows that the addition of Nickel significantly promotes the activity and selectivity of the catalyst K_2MoO_4/SiO_2 (dried). In the presence of Ni-modified catalyst K_2MoO_4/Ni-SiO_2 (dried), the carbon monoxide conversion, selectivity to methanethiol and the yield of methanethiol were, respectively, found to reach as high as 62.0, 42.2 and 26.2%, accompanying with 5% decreasing in selectivity to CO_2. It was found that the conversion of CO and the selectivity to methanethiol increased firstly with increasing the Nickel content of the catalyst, then kept at a nearly constant level when the content of Nickel was in the range of 0.44–0.82%. However, when the nickel content increased over 1.1%, the selectivity to mathanethoil inversely decreased, implying that overloading of Ni on SiO_2 leads to attenuating the activity of the catalysts. Meanwhile, the catalyst K_2MoO_4/Ni-SiO_2 calcined at 673 K exhibited slightly lower activity and selectivity under the same reaction conditions.

Figure 1 shows the effect of K_2MoO_4 loading on catalytic performance of the catalyst K_2MoO_4/Ni-SiO_2 (12/0.64/100). As the increase of K_2MoO_4 loading, the conversion of CO increased first, then lowered; when the loading of K_2MoO_4 increased to 12%, the conversion reached a maximum value, being as high as 60.7%. At the same time, the selectivity toward by-product CO_2 reached maximum level as well. Further increasing the loading of K_2MoO_4 led to the decrease of the activity. However, the maximum selectivity

Table 2 Performance of different catalysts for methanethiol synthesis from H_2S-rich synthesis gas

Catalyst ($MoO_3\% = 12\%$)	CO conversion (%)	Product selectivity yield (%)					Yield (%)
		Hydrocarbon		COS	CO_2	CH_3SH	CH_3SH
		C_1	C_2				
K_2MoO_4[a]/SiO_2							
12/100 (dried)	18.8	T	T	20.0	48.9	31.1	5.8
K_2MoO_4/Ni-SiO_2							
12/0.10/100 (dried)	44.4	0.02	T	19.3	42.3	38.4	17.0
12/0.21/100 (dried)	55.1	0.02	T	16.1	43.4	40.5	22.3
12/0.44/100 (dried)	62.0	0.03	T	14.5	43.3	42.2	26.2
12/0.64/100 (dried)	60.7	0.03	T	14.6	43.2	42.2	25.6
12/0.82/100 (dried)	60.4	0.04	T	14.5	43.5	41.9	25.3
12/0.82/100 (calcined at 673 K)	53.5	0.03	T	17.1	45.6	37.2	19.9
12/1.10/100 (dried)	59.7	0.04	T	16.7	43.8	39.5	23.4

The data in Table 2 were obtained when the steady state had reached

Reaction conditions: $CO:H_2S:H_2 = 1:2:1$, $P = 0.2$ MPa, $T = 573$ K, GHSY = 2,000 h^{-1}

[a] The amount of MoO_3 was taken to express that of K_2MoO_4 (wt%) *T*: trace <0.01%

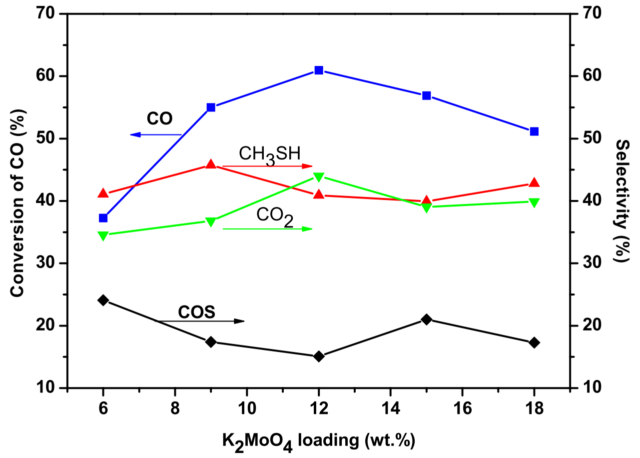

Fig. 1 Effect of the K_2MoO_4 loading on catalytic performance of the catalyst K_2MoO_4/Ni-SiO_2 (12/0.64/100). Reaction conditions: $CO:H_2S:H_2 = 1:2:1$, $P = 0.2$ MPa, $T = 573$ K, GHSY = 2,000 h^{-1} 109 × 86 mm (600 × 600 DPI)

to main product mathenethiol occurred when the K_2MoO_4 loading was 9%, where the lowest selectivity to CO_2 was found. Interestingly, the varying regularity of the selectivity to carbon sulfide as a function of K_2MoO_4 loading is just the same as that of mathenethiol. This suggests that carbon dioxide and methanethoil are derivatives of carbon sulfide, which are, respectively, formed by the hydrolysis and hydrogenation of carbon sulfide, which is in line with the results reported in the literatures [6, 7].

The catalytic performance of the catalyst K_2MoO_4/Ni-SiO_2 (12/0.82/100) for methanethiol synthesis after thermal treatment at 673 K in H_2S-rich synthesis gas as a function of treatment time is presented in Table 3. Compared with the catalyst K_2MoO_4/Ni-SiO_2 (12/0.82/100) without thermal treatment, after 2 h thermal treatment, the carbon monoxide conversion, selectivity to methanethiol and the yield of methanethiol were found to be decreased by 5, 2.2 and 3.3%, respectively, accompanying with 1.9% increasing in selectivity to CO_2. Over 4 h thermal treatment, the catalytic activity of the catalyst was no longer reduced, but the activity was still lower than that of the catalyst without thermal treatment. This suggests that thermal treatment led to the decay of the catalytic performance of the catalyst.

3.2 BET Study

BET characterization results of different supports and catalysts are listed in Table 4. The BET characterization results of Ni-modified SiO_2 are similar to those of unmodified SiO_2, this illustrates that the surface properties of SiO_2 are not changed much by a small amount of nickel electrolessly plated. Compared the surface properties of catalyst K_2MoO_4/Ni-SiO_2 with those of K_2MoO_4/SiO_2, it was found that BET area, pore size and pore volume of the former were all bigger than those of the latter. It may be inferred that the K_2MoO_4 species dispersed on the Ni-modified SiO_2 surface were slightly smaller than those directly dispersed on the SiO_2.

3.3 LRS Study

Raman spectra of unsupported and supported K_2MoO_4 catalysts dried (and calcined at 673 K for 5 h in air) at 383 K for 10 h in air are shown in Fig. 2.

The Raman peaks occurred at 317, 821, 852 and 888 cm^{-1} (shown in Fig. 2a) can be ascribed to unsupported

K_2MoO_4 [15]. The spectra of K_2MoO_4/Ni-SiO_2 (see Fig. 2b) with different nickel contents appeared at 220, 486, 857, 892 and 928 cm^{-1}, while no NiO characteristic band (497 cm^{-1}) was detected, suggesting that promoter nickel species on the catalysts K_2MoO_4/Ni-SiO_2 may be in the form of metal nickel deposited by electroless plating. The band at 486 cm^{-1} can be assigned to fourfold siloxane rings from silica [16]. Because the acidity of the solution became a little more on drying, MoO_4^{2-} species normally present in basic solution are polymerized to $Mo_2O_7^{6-}$ or $Mo_7O_{24}^{6-}$species [15, 17]. The bands at 928 and 220 cm^{-1} are therefore consistent with that specific to dimolybdate species [15], while the band at 928 cm^{-1} may arise from the shifting of the band at 943 cm^{-1} to lower wave number, suggesting that the interaction of molybdate species with the support surface and/or surrounding nickel species takes place [18]. Meanwhile, the bands at 857 and 892 cm^{-1} can be, respectively, assigned to surface tetrahedral and monomeric tetrahedral molybdate species [15, 17, 19]. Obviously, the spectra originating from supported K_2MoO_4 catalyst are totally different from that of unsupported K_2MoO_4 due to the interaction of the active component with the support and/or the promoter nickel [20].

Fig. 2 Raman spectra of K_2MoO_4 (**A**) 98 × 86 mm (600 × 600▶ DPI). **B** Raman spectra of the catalysts K_2MoO_4/Ni-SiO_2 dried at 383 K for 10 h in air: *a* K_2MoO_4/SiO_2(12/100); *b* K_2MoO_4/Ni-SiO_2(12/0.21/100); *c* K_2MoO_4/Ni-SiO_2(12/0.44/100); *d* K_2MoO_4/Ni-SiO_2(12/0.64/100); *e* K_2MoO_4/Ni-SiO_2(12/1.10/100) 98 × 86 mm (600 × 600 DPI). **C** Raman spectra of the catalysts K_2MoO_4/Ni-SiO_2 calcined at 673 K for 5 h in air: *a* K_2MoO_4/SiO_2(12/100); *b* K_2MoO_4/Ni-SiO_2(12/0.21/100); *c* K_2MoO_4/Ni-SiO_2(12/0.44/100); *d* K_2MoO_4/Ni-SiO_2(12/0.64/100); *e* K_2MoO_4/Ni-SiO_2(12/1.10/100) 98 × 86 mm (600 × 600 DPI)

Table 4 BET measurement results of different supports and catalysts

Catalysts (30–45 m)	BET area (m^2/g)	Pore size (nm)	Pore volume (cc/g)
SiO_2	256.67	12.13	0.99
Ni-SiO_2(Ni content%)			
0.49	252.87	10.31	0.96
0.71	247.61	12.12	0.96
0.91	249.36	12.13	0.97
1.17	248.84	12.13	0.96
K_2MoO_4/SiO_2			
20/100	132.38	12.13	0.55
K_2MoO_4/Ni-SiO_2			
12/0.21/100 (dried)	134.03	12.13	0.62
12/0.44/100 (dried)	136.89	12.12	0.63
12/0.64/100 (dried)	138.34	14.67	0.64
12/0.82/100 (dried)	139.65	14.68	0.65
12/0.82/100 (calcined)	143.01	13.05	0.61
12/1.1/100 (dried)	140.57	14.68	0.63

After calcination, the main Raman signals arising from the catalysts K_2MoO_4/Ni-SiO_2 shifted towards lower wave numbers (Fig. 2c) from 928 to 893 cm^{-1} in comparison with those of uncalcined catalysts, suggesting that the molybdate species on the surface of the catalysts after calcination exist mostly in the form of monomolybdate (Td) [19]. There are three Raman bands arising from K_2MoO_4/SiO_2, which occurred at 317, 893 and 937 cm^{-1} (Fig. 2c–a), respectively. The bands at 317 and 893 cm^{-1} can be assigned to K_2MoO_4 species, while the band at 937 cm^{-1} can be attributed to dimolybdate species. Raman spectra of the calcined catalysts K_2MoO_4/Ni-SiO_2 showed two strong bands at 317 and 893 cm^{-1} accompanying with several small bands at 216, 818, 850, 922 and 930 cm^{-1} (Fig. 2C-b–e), of which the bands at 317 and 893 cm^{-1} were also attribute to K_2MoO_4 species, corresponding to the vibration model of δ(Mo–O) and $v_{s.}$(Mo–O), respectively. The bands at 930 and 216 cm^{-1} may be assigned to small tetrahedral Mo species containing potassium component [21, 22], While the intensity of the band at

Table 3 The activity data of K_2MoO_4/Ni-SiO_2 catalyst after thermal treatment at 673 K

Catalyst (MoO_3% = 12%)	CO conversion (%)	Product selectivity (%)					Yield (%)
		Hydrocarbon		COS	CO_2	CH_3SH	CH_3SH
		C_1	C_2				
$K_2MoO_4^a$/Ni-SiO_2							
12/0.82/100							
0 h	60.4	0.04	T	14.5	43.5	41.9	25.3
2 h	55.4	0.05	T	14.9	45.4	39.7	22.0
4 h	53.9	0.05	T	13.0	48.1	38.9	21.0
6 h	53.9	0.05	T	12.9	49.1	39.0	21.0

The data in Table 3 were obtained when the steady state had reached

Reaction conditions: $CO:H_2S:H_2 = 1:2:1$, $P = 0.2$ MPa, $T = 573$ K, GHSY = 2,000 h^{-1}

[a] The amount of MoO_3 was taken to express that of K_2MoO_4 (wt%) *T*: trace <0.01%

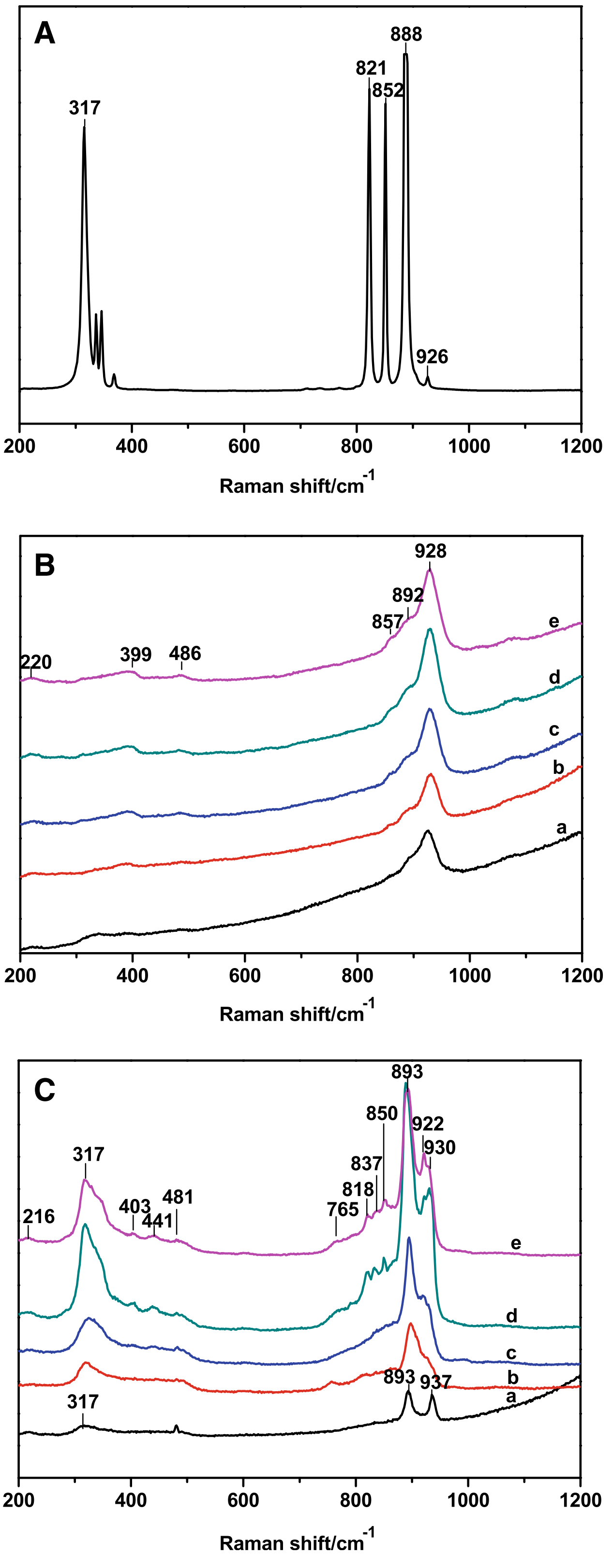

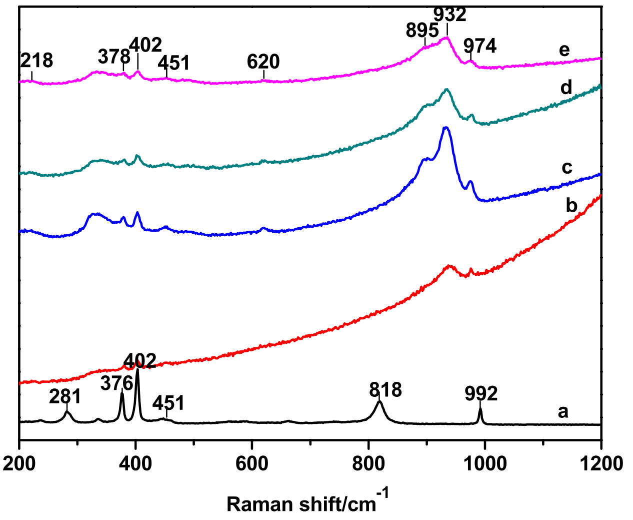

Fig. 3 Raman spectra of the catalysts after reaction for 5 h: *a* MoS_2 (*pure*); *b* K_2MoO_4/SiO_2(12/100); *c* K_2MoO_4/Ni-SiO_2(12/0.44/100); *d* K_2MoO_4/Ni-SiO_2(12/0.64/100); *e* K_2MoO_4/Ni-SiO_2(12/1.10/100) 98 × 86 mm (600 × 600 DPI)

922 cm^{-1} was attribute to a distorted [MoO_4] tetrahedron on the support [23]. It was found that the intensities of the bands at 893 and 922 cm^{-1} became stronger as increasing the nickel content, suggesting that the promoter nickel facilitated the monomolybdate species formation.

Raman spectra of the catalysts after reaction in H_2S-rich synthesis gas are presented in Fig. 3. From Fig. 3 five vibration bands specific to MoS_2 (*pure*) at 281, 376, 402, 818 and 992 cm^{-1} can be detected (see Fig. 3a). The strong bands at 376 and 402 cm^{-1} were assigned to the vibration of Mo = S for MoS_2 species [23]. While the smaller ones at 281, 818 and 992 cm^{-1} can be attributed to MoO_3, which was inferred to arise from the reoxidation of MoS_2 surface species by ambient oxygen under the action of the heat from the laser [23, 24]. There appeared some bands at 218, 620, 895, 932 and 974 cm^{-1} besides 378 and 402 cm^{-1} for the sulfided K_2MoO_4/Ni-SiO_2 catalysts (shown in Fig. 3b–e). The bands at 378 and 402 cm^{-1} should be assigned to MoS_2 species, although the bands are broad due to the sulfur-for-oxygen exchange. Meanwhile, the intensities of the signals arising from MoS_2 species decreased as the increase of nickel content, suggesting that more promoter nickel may lead to restrain the formation of MoS_2 species on the surface during the sulfiding process of the catalyst K_2MoO_4/Ni-SiO_2, interpreting its lower hydrosulfurizaton activity (see Table 2). On the other hand, the bands at 895 cm–^{1}, 932 cm–^{1} and 974 cm–^{1} can be attributed to reduced and/or sulfided molybdenum species which interact with oxygen and/or nickel cation to give out strong Raman signals [23]. According to their activity results, the bands appeared at 451 and 620 cm^{-1}, which are due to molybdenum oxysulfides [23], were not detected yet for the sulfided catalyst K_2MoO_4/SiO_2, so the molybdenum oxysulfides can be considered to be active species for this reaction.

3.4 TPR Study

Figure 4 shows the TPR profiles of different catalysts calcined at 673 K for 5 h in argon. In Fig. 4a, only a main reduction peak at about 887 K with a shoulder at about 756 K is detected. Studied the TPR behavior of Mo/C and K-promoted molybdate catalysts, Feng et al. [25] have found that there were two positive reduction peaks which are simply assigned to the reduction of Mo^{6+} to Mo^{4+} and Mo^{4+} to Mo^0, respectively. They have also pointed out that for K-Mo/C catalysts, K itself can not be reduced but modify the reducibility of other metal compounds. Wang [26] has recently reported that for the TPR behavior of $MoO_3/K/SiO_2$ catalysts calcined at 773 K in air there are two reduction peaks, the one at about 770 K is attributed to the reduction of octahedral molybdate Mo (Oh), the other at about 1,000 K is assigned to the tetrahedral molybdate Mo (Td) reduction. According to the LRS characterization results, the main reduction peak at 887 K and the shoulder reduction peak at about 756 K can be ascribed to the reduction of the K_2MoO_4 species and dimolybdate species, respectively. Compared with Fig. 4a, the major reduction peak arising from the catalyst K_2MoO_4/Ni-SiO_2 shifted towards 756 K, which may be assigned to the reduction of well-dispersed and (or) distorted species of K_2MoO_4 from Mo^{6+} to Mo^{4+}. As compared with K_2MoO_4/SiO_2, the main reduction peak temperature of K_2MoO_4/Ni-SiO_2 reduced by about 131 K, suggesting that K_2MoO_4 species of the catalyst K_2MoO_4/Ni-SiO_2 were more easily reduced to low-valence Mo species, which may be more advantageous for improving the conversion of carbon monoxide.

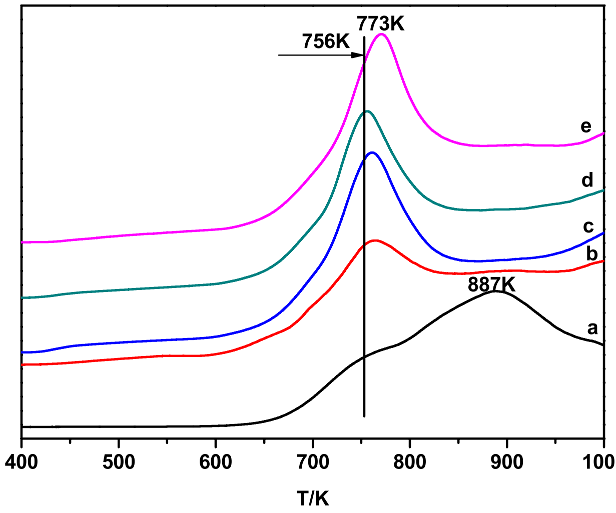

Fig. 4 TPR profiles of catalysts calcined at 673 k for 5 h in argon: *a* K_2MoO_4/SiO_2(12/100); *b* K_2MoO_4/Ni-SiO_2(12/0.21/100); *c* K_2MoO_4/Ni-SiO_2(12/0.44/10); *d* K_2MoO_4/Ni-SiO_2(12/0.64/100); *e* K_2MoO_4/Ni-SiO_2(12/1.10/100) 98 × 85 mm (600 × 600 DPI)

It was also noted that when the nickel content of the catalyst K_2MoO_4/Ni-SiO_2 arrived at 1.10%, the low temperature peak shifted from 756 to 773 K higher by 17 K, this might be related with more tetrahedral molybdate species on the catalyst K_2MoO_4/Ni-SiO_2 (12/1.10/100) surface, which were considered to be more difficult to be reduced.

4 Conclusions

Small amount of nickel deposited onto support SiO_2 by electroless plating greatly improves the catalytic performance of the catalyst K_2MoO_4/Ni-SiO_2 for methanethiol synthesis from H_2S-rich synthesis gas. As compared with K_2MoO_4/SiO_2 catalyst, K_2MoO_4/Ni-SiO_2 catalyst exhibits higher conversion of carbon monoxide and higher selectivity to methanethiol, but lower selectivity to carbon dioxide. After thermal treatment the catalyst showed lower catalytic performance in comparison with the one without thermal treatment. BET results revealed K_2MoO_4 species dispersed better on the surface of Ni-SiO_2 than directly on SiO_2. Raman characterization results showed that as the nickel content increased, the intensities of Raman signals arising from dimolybdate species increase for the dried catalysts, while those of the peaks arising from molybdate MoO_4^{2-} increase for the calcined ones. For the sulfided catalysts K_2MoO_4/Ni-SiO_2, there appeared some characteristic bands arising from MoS_2, reduced molybdenum, molybdenum oxysulfides, but no signal originating from molybdenum oxysulfides for the sulfided catalyst K_2MoO_4/SiO_2 was detected. Raman signals arising from NiO did not occur on the dried or calcined catalysts K_2MoO_4/Ni-SiO_2 surfaces. TPR testing results indicated that the main reduction peak temperature of K_2MoO_4/Ni-SiO_2 reduced by about 131 K in comparison with that of K_2MoO_4/SiO_2 catalyst. With the nickel content increasing, the main reduction peak temperature slightly shifted to high temperature due to more tetrahedral coordinated molybdate Mo (Td) on the catalyst surface occurring.

Acknowledgments The authors gratefully acknowledge Degussa GmbH (Germany) for financial support.

References

1. Buchholz B (1983) US Patent 4,410,731
2. Haines PG (1984) US Patent 4,449,006
3. Ratcliffe CT, Tromp PJ, Wachs IE (1986) US Patent 4,570,020
4. Boulinguiez M, Forquy C, Barrault J (1987) US Patent 4,665,242
5. Chersich CC, Wachs IE (1986) EP0167354
6. Barrault J, Boulinguize M, Forquy C, Maurel R (1987) Appl Catal 33:309
7. Mul G, Wachs IE, Hirschon AS (2003) Catal Today 78:327

8. Zhang BJ, Taylor SH, Hutchings GJ (2003) Catal Lett 91:181
9. Yang YQ, Wang Q, Lin RC, Zhang HB (2005) WO2005040082
10. Zh L, Yi Chen (1998) J Catal 177:314
11. Tsai TK, Chuang CC, Chao CG, Liu WL (2003) Diamond Relat Mater 12:1453
12. Liu WL, Chen WJ, Tsai TK, Hsieh SH, Chang SY (2007) Appl Surf Sci 253:3843
13. Dai HB, Liang Y, Wang P, Yao XD, Rufford T, Lu M, Cheng HM (2008) Int J Hydrogen Energy 33:4405–4412
14. Chen AP, Wang Q, Hao YJ, Fang WP, Yang YQ (2007) Catal Lett 118:295
15. Erdöhelyi A, Fodor K, Solymosi F (1997) J Catal 166:244
16. Cheng CP, Schrader GL (1979) J Catal 60:276
17. Kantschewa M, Delannay F, Jeziorowski H, Delgado E, Eder S, Ertl G, Knözinger H (1984) J Catal 87:482
18. Damyanova S, Spojakina A, Jiratova K (1995) Appl Catal A Gen 125:257
19. Williams CC, Ekerdt JG, Jehng JM, Hardcastle FD, Turek AM, Wachs IE (1991) J Phys Chem 95:8781
20. Verbruggen NFD, von Hippel LMJ, Mestl G, Lengeler B, Knözinger H (1994) Langmuir 10:3073
21. Kim DS, Segawa K, Soeya T, Wachs IE (1992) J Catal 136:539
22. Jiang M, Bian GZh, Li F, Fu YL (1994) J Catal 146:144
23. Schrader GL, Cheng CP (1983) J Catal 80:369
24. Lewis IR, Edwards HGM (2001) Handbook of Raman Spectroscopy from the research laboratory to the process line, USA p. 814
25. Feng L, Li XG, Dadyburjor DB, Kugler EL (2000) J Catal 190:1
26. Wang Q (2007) Ph.D thesis, University of Xiamen in China